Seismic performance analysis of a smart base-isolation system considering dynamics of MR elastomers

HYUNG-JO JUNG,[1] SEUNG-HYUN EEM,[1] DONG-DOO JANG[1] AND JEONG-HOI KOO[2]

[1]*Civil and Environmental Engineering Department, KAIST, Daejeon, South Korea*

[2]*Mechanical and Manufacturing Engineering Department, Miami University, Oxford, Ohio, USA*

ABSTRACT: This article investigates a smart base-isolation system using magnetorheological (MR) elastomers, which are a new class of smart materials whose elastic modulus or stiffness can be adjusted depending on the magnitude of the applied magnetic field. The primary goals of this study are to develop a smart base-isolation model that represents the field-dependent dynamic behaviors of MR elastomers, to design and construct a scaled smart isolation system and a scaled building structure for a proof of concept study and to investigate the dynamic performance of the smart base-isolation in mitigating excessive vibrations of the scaled building structure under earthquake loadings. To this end, a dynamic model of an MR elastomer was first obtained based on characteristic test results of MR elastomers in shear mode. The dynamic model was then incorporated in a shear building model. Its effectiveness was validated by comparing the test results of a small-scale, single-story building structure coupled with the MR elastomer under harmonic excitations. After validating the MR elastomer-based base-isolation system, a further numerical study was performed to evaluate its effectiveness under seismic excitations. The results show that the proposed MR elastomer base-isolation system with the fuzzy logic control algorithm outperforms the conventional passive-type base isolation system in reducing the responses of the building structure for the seismic excitations considered in this study. The results further suggest that the feasibility of using MR elastomers as variable stiffness elements for enhancing the performance of conventional base-isolation systems.

Key Words: MR elastomer, smart base-isolation, seismic performance, numerical simulation.

Introduction

THE control strategies used for civil engineering structures, such as buildings and bridges, can be divided into three categories: (1) energy dissipation, (2) energy transfer, and (3) base isolation. The base isolation method, in which base isolation devices are inserted between the ground and a superstructure, is one of the most promising structural control techniques to mitigate the structural responses in the event of an earthquake. Many passive-type base-isolation techniques (e.g., laminated rubber bearings, lead-rubber bearings, friction bearings, etc.) have been implemented to full-scale buildings and bridges because of their simplicity, economic effectiveness, inherent stability, and reliability (Spencer et al., 2003). However, there exist several disadvantages of the passive-type base-isolation methods such as large seismic gaps and poor adaptability to various ground excitations.

To address the aforementioned problems of passive systems, in recent years, a considerable attention has been given to "smart" base-isolation systems (Ramallo et al., 2002; Yoshioka et al., 2002), which is the combination of the passive-type base-isolation device and the semiactive control device, such as, magnetorheological (MR) dampers. When compared with conventional systems, the smart base-isolation systems can achieve high-control performance as well as good adaptability to variations in ground excitations. Among various semiactive control devices, MR dampers have been actively studied as semiactive actuators for smart base-isolation systems. Recently, a new smart base-isolation system, MR elastomers, or MR elastomers used isolation systems have been proposed (Koo et al., 2008; Jung et al., 2009). MR elastomers are the solid-type analog of the MR fluids. They can be viewed as ordinary elastomeric bearings with a variable stiffness, which can be controlled according to the real-time response of the structure by varying the applied magnetic field. Therefore, the fundamental natural period of the base-isolated structure can be changed in real time to avoid the coincidence with the earthquake period, resulting in the considerable

*Author to whom correspondence should be addressed.
Email: hjung@kaist.ac.kr
Figures 2, 4, 5, 7–9, 11, and 12 appear in color online: http://jim.sagepub.com

1045-389X/11/00 0001–12 $10.00/0 DOI: 10.1177/1045389X11414224

mitigation of excessive structural vibrations. To effectively protect a structure from seismic activities, the horizontal responses (such as interstory drifts) of the structure should be reduced. Conventional elastomeric base-isolation systems rely on the shear deformation of the elastomeric bearings to decouple the structure from the horizontal ground motions. Similarly, the MR elastomers operate in shear mode with variable shear modulus or stiffness depending on the applied magnetic field. Note that operating MR elastomers offers a larger MR effect (change in stiffness with and without magnetic field) when compared with its compression mode. As controllable stiffness elements, MR elastomers have already been applied in adaptive vibration absorbers (Deng and Gong, 2007) and tunable vibration isolators (Opie and Yim, 2009). However, there has been limited research on the application of MR elastomers for base-isolation systems and civil engineering structures.

In an attempt to investigate the feasibility of using MR elastomers in base-isolation systems, this study intends to evaluate the seismic performance of a smart base-isolation system based on MR elastomers. To this end, a dynamic model of MR elastomers is first developed using shear deformation test results of MR elastomer samples. This dynamic model is then incorporated in the smart base-isolation system to represent realistic field-dependent behaviors of MR elastomers. To validate the performance of the smart isolation system, a scaled single-story building structure coupled with the MR elastomer is designed and tested using a shaking table under harmonic excitations. The experimental results are compared with the equivalent numerical model. After experimentally validating the structure model coupled with the smart base-isolation system, a further numerical study is performed to assess the effectiveness of the MR elastomer-based, smart base-isolation system under seismic excitations.

MR elastomer-based smart base isolation

MR elastomers are composite materials consisting of micron-sized iron particles and a non-magnetic medium (e.g., silicon, rubber, etc.). MR elastomers are, therefore, a class of smart materials whose elastic modulus of stiffness can be varied depending on the magnitude of the applied magnetic field by aligning iron particles along the direction of the magnetic field, as shown in Figure 1.

Figure 2 shows an MR elastomer-based base-isolation system coupled with a structure. The arrows in the figure indicate that the stiffness of MR elastomers is controllable depending on the magnitude of input magnetic flux density, which is determined by structural responses and ground motions measured by the sensors. Thus, unlike

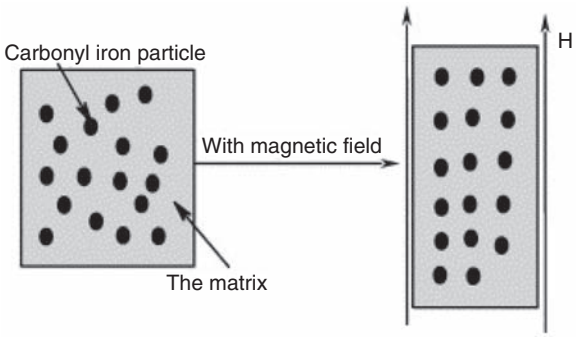

Figure 1. *Schematic representation of MR elastomers (Wang et al., 2007).*

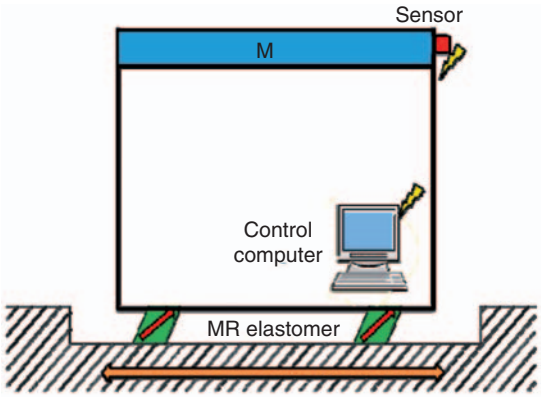

Figure 2. *A structure model coupled with an MR elastomer-based base-isolation system.*

the passive-type base-isolation system, the controllable MR elastomer allows the base-isolation system to adapt to various loading conditions, effectively reducing the excessive structural vibrations. The excessive structural vibrations can occur when the frequency of the ground excitation coincides with the fundamental frequency of the structure and also can occur when the ground excitation frequency is close to the natural frequency of a passive or conventional base-isolation system. In this case, the passive-type isolation system installed in the base of a structure can indeed cause harmful structural vibrations (Mendoza et al., 1988). Therefore, a controllable stiffness base-isolation system would effectively protect the structure from excessive resonant vibrations by shifting the natural frequency of the system in response to the ground motions.

Dynamic model for MR elastomer

To develop a dynamic model of MR elastomers, this study uses the experimental characterization results of MR elastomer samples that authors published (Jung et al., 2009). In developing a dynamic model, this study combines a Bouc–Wen model with spring and

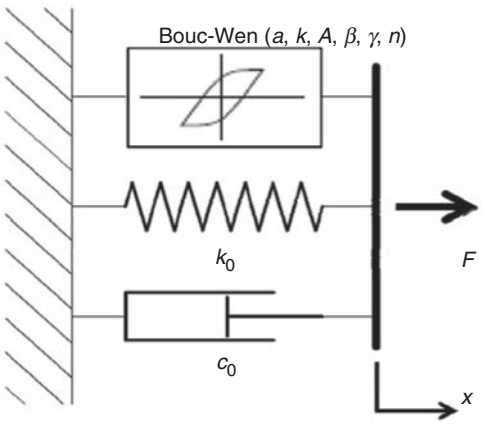

Figure 3. *Bouc–Wen model of MR elastomer.*

dashpot elements as shown in Figure 3. The Bouc–Wen model is often used to describe non-linear hysteretic systems. The detailed modeling of non-linear hysteretic systems using the laws of physics is an arduous task, and the obtained models are often too complex to use in practical applications. In contrast, the Bouc–Wen model, in general, does not come from the detailed analysis of the physical behavior of systems with hysteresis (Mohammed et al., 2009). Moreover, the Bouc–Wen model has been widely used to describe field-dependent hysteric behaviors and other complex dynamic characteristics of systems, such as MR dampers, wood joints, and base-isolation devices for buildings (Faycal et al., 2007).

Equation (2) and (3) show the mathematical expressions for the proposed MR elastomer force model, which consists of a spring, a dashpot, and the Bouc–Wen model. The Bouc–Wen model consists of parameters a, k, A, β, γ, and n. To determine the parameter values for the proposed model, an optimization procedure is used. The inputs to the optimization routine are the displacement, velocity, and acceleration of MR elastomer deformation, the magnetic flux density, and the exciting frequency. The output data are the difference between the measured force from characterization experiments and the predicted force of the model. The optimization procedure is based on the iterative prediction-error minimization method, which uses a non-linear gray-box model to describe the system behavior as a set of non-linear ordinary differential or difference equations with unknown parameters. The optimal criterion is minimizing $\det(E' \cdot E)$, where E represents the prediction error. This is the optimal choice in a statistical sense and leads to the maximum likelihood estimates in case nothing is known about the variance of the noise.

$$E = \sum_{t=0} e^2(t), \tag{1}$$

where $e(t)$ is the difference between the measured output and the predicted output of the model.

The force in the proposed MR elastomer dynamic model is given by:

$$F = am_0\ddot{x} + (1+a)m_0 q + k_0 x + c_0\dot{x}, \tag{2}$$

where the evolutionary variable q is governed by:

$$\dot{q} = \ddot{x}(A - (\beta \text{sign}(\ddot{x}q) + \gamma) \cdot |q|^n). \tag{3}$$

A set of parameters is determined to fit the response of the MR elastomer model to the experimentally measured response of the MR elastomer (Jung et al., 2009). MR elastomer samples were fabricated by curing a two-component elastomer resin with 30% content of 10-μm-sized iron particles by volume in a rectangular prism mold $19.05 \times 12.7 \times 12.7$ mm^3(Jung et al., 2009). For the iterative process, the initial values for k_0 and c_0 are assumed based on the test results and the other parameters are all set 1. The final values of the parameters for the model in Equations (2) and (3) are as follows:

$$a = -1.12,\ m_0 = 12 \text{ kg},\ \beta = 19 \text{ sec}^4/\text{m}^2,\ A = 60,$$
$$\gamma = 0,\ n = 2,$$

$$k_o = 21020 + 19970\,B + 9697\,f - 19730\,B^2 + 8917\,Bf - 5568\,f \quad 38080\,B^3 - 9655\,B^2 f, - 2142\,Bf^2 831.1\,f^3 \text{ (N/m)}$$

$$c_o = 1487\,B^{0.2213} f^{-0.9761} + 310.4 \text{ (N} \cdot \text{sec/m)}.$$

In the above equations, B means the applied magnetic flux density, f means the frequency, k_0 represents the variation in stiffness due to the magnetic field, c_0 represents the variation in dashpot due to the magnetic field, and $x(t)$ is the deformation of MR elastomers or the base displacement. The additional force $F(t)$ can be varied with the command input B, calculated from control algorithms. This model is built and verified within the range of less than 3 mm for the displacement and less than 0.52 T for the applied magnetic flux density (which is the maximum achievable value in the experiment).

After obtaining the optimal values for the dynamic model, its effectiveness is validated by comparing the dynamic behaviors of the MR elastomer model with the results of the shear-mode test using the MR elastomer sample (Jung et al., 2009) as shown in Figures 4 and 5. The figures show that sample comparison results between the simulation and the experiment, where the minimum and maximum magnetic fields are applied. The results show that the output force curves generated by the model coincide well with the experimental results. Moreover, the results are quite consistent with different magnetic flux density cases.

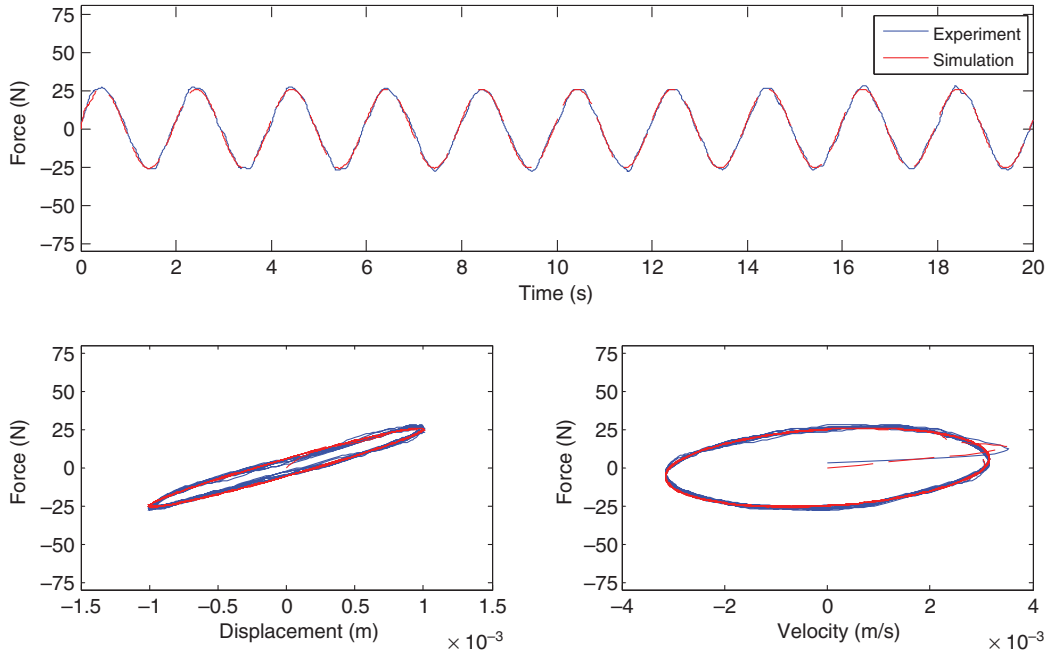

Figure 4. *Comparison between the results of simulation and experimental test (sinusoidal displacement = 0.5 Hz and a constant applied B = 0.05 T).*

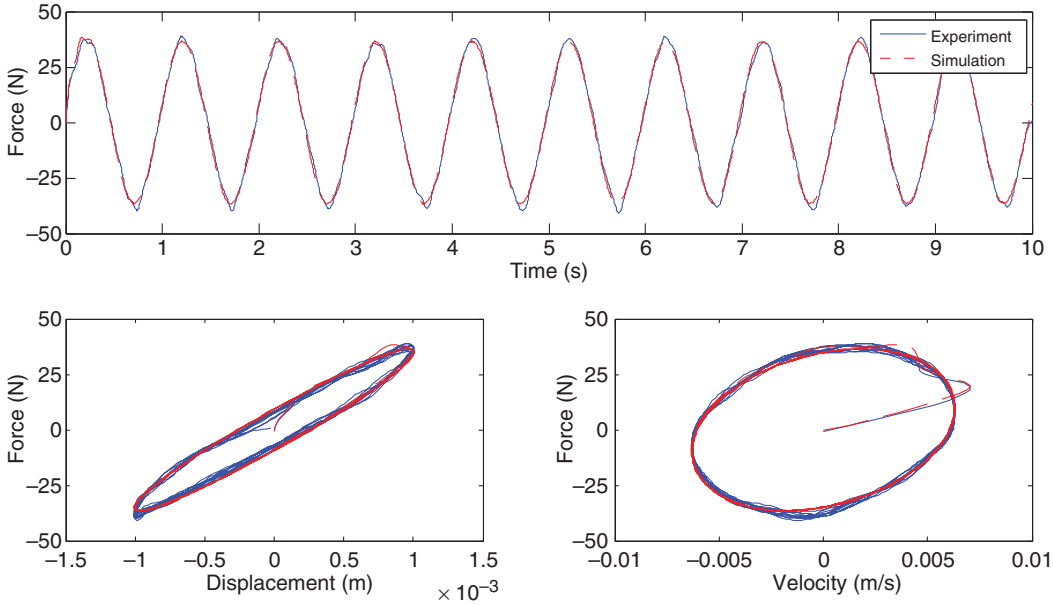

Figure 5. *Comparison between the results of simulation and experimental test (sinusoidal displacement = 1 Hz and a constant applied* B = *0.5 T).*

Experimental validation of the MR elastomer base-isolation system

To validate the performance of the proposed MR elastomer model and MR elastomer-based base-isolation system, an experimental study is carried out, and the performance results of the MR elastomer system are compared with those of an equivalent numerical model. For the experimental study, a test setup is designed and constructed. The setup consists of a small-scale test structure, two MR elastomer base isolators, and electromagnets. Mounted on a shaking table, the structure setup is tested under harmonic base input motions. The dynamic performance of the MR elastomer base-isolation system in reducing structural responses is then compared with that of the numerical model, which consists of an equivalent

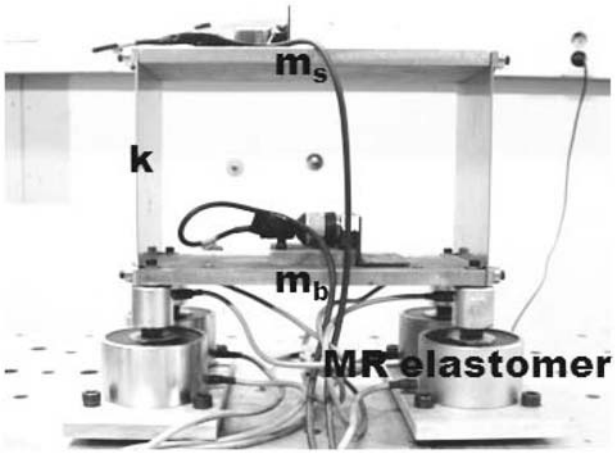

Figure 6. *Experimental structure (Smart base-isolation system).*

Table 1. Structural parameters of the structure model.

Parameter	Value
Mass (kg) of base (m_b)	7.757
Mass (kg) of top (m_s)	6.780
Stiffness (kN/m)	40.180

structure model and the MR elastomer model developed in the previous section. After the validation and evaluation of the MR elastomer system, the numerical model will be used for further seismic performance analysis of the proposed smart base-isolation system using scaled historic earthquake inputs in a later section.

Experimental evaluation

Figure 6 shows the scaled single-story shear building structure sits atop MR elastomer-based isolation systems. The MR elastomers are placed between two electromagnets at each of the four corners. The electromagnets can adjust the magnitude of the magnetic flux density across the MR elastomers (from 0.01 T at the minimum input current (0 V) to 0.52 T at the maximum input current (90 V), resulting in change of the stiffness of the MR elastomers. A shaking table system is used to provide the input excitations, and the acceleration and interstory drift of the structure and the isolator deformation are measured using accelerometers as well as laser displacement sensors. The parameters of the test structure are shown in Table 1.

For the experimental evaluation of the structure, the shaking table system provided harmonic input excitations (a sinusoidal signal with the amplitude of 10 mm and the frequency of 3 Hz). Three cases of harmonic test are performed with the minimum/maximum magnetic flux density and one in between the maximum and the minimum values ($B = 0.01$ T, 0.16 T, and 0.52 T). As shown in Figure 7, the structural responses are reduced as the magnetic flux density increases. Table 2 summarizes the amplitude values of the structural responses for the three different test cases. In the table, the values in parenthesis represent the reduction of the structural responses compared with the minimum magnetic flux density case ($B = 0.01$ T).

Numerical evaluation

In this section, a 2-DOF (degree of freedom) structural model coupled with a MR elastomer-based base-isolation system is considered for validating the effectiveness of the MR elastomer dynamic model. The building structure model used in this study is equivalent to the test structure. Adding the isolation layer to the structural model, the whole structural model can be treated as a 2-DOF system, as shown in Figure 8. In the figure, m_s, k_s, and c_s denote the story mass, stiffness, and damping coefficient of the structure, respectively, and m_b, k_b, and c_b represent the mass of the isolation layer, the stiffness, and the damping coefficient of the base isolator, respectively. The structural parameter values used in the simulation are the same physical values as the experimental structure (see Table 1). The variable stiffness of the MR elastomers is represented as $k_b(t)$.

Assuming the structural motion is sufficiently small such that non-linear effects may be neglected, and denoting the base and structure displacements relative to the ground by x_b and x_s, respectively, the equations of motion of the base-isolated system may be expressed as:

$$M\ddot{x} + C\dot{x} + K(t) = -M\Gamma\ddot{x}_g \tag{4}$$

or

$$M\ddot{x} + C\dot{x} + K_0 x = \Lambda f - M\Gamma\ddot{x}_g, \tag{5}$$

where x ($x = \begin{bmatrix} x_b & x_s \end{bmatrix}^T$) is the displacement vector of the structure and base isolator; M, C, and K are the mass, damping, and stiffness matrices, respectively; f is the supplemental force exerted by the MR elastomers, $\Lambda = \begin{bmatrix} 1 & 0 \end{bmatrix}^T$ represents the position of the supplemental force ; Γ is the unity vector; $\ddot{x}_g$ is the ground acceleration. The system matrices can be expressed as:

$$M = \begin{bmatrix} m_b & 0 \\ 0 & m_s \end{bmatrix}, \; C = \begin{bmatrix} c_b + c_s & -c_s \\ -c_s & c_s \end{bmatrix},$$
$$K_0 = \begin{bmatrix} k_b + k_s & -k_s \\ -k_s & k_s \end{bmatrix}.$$

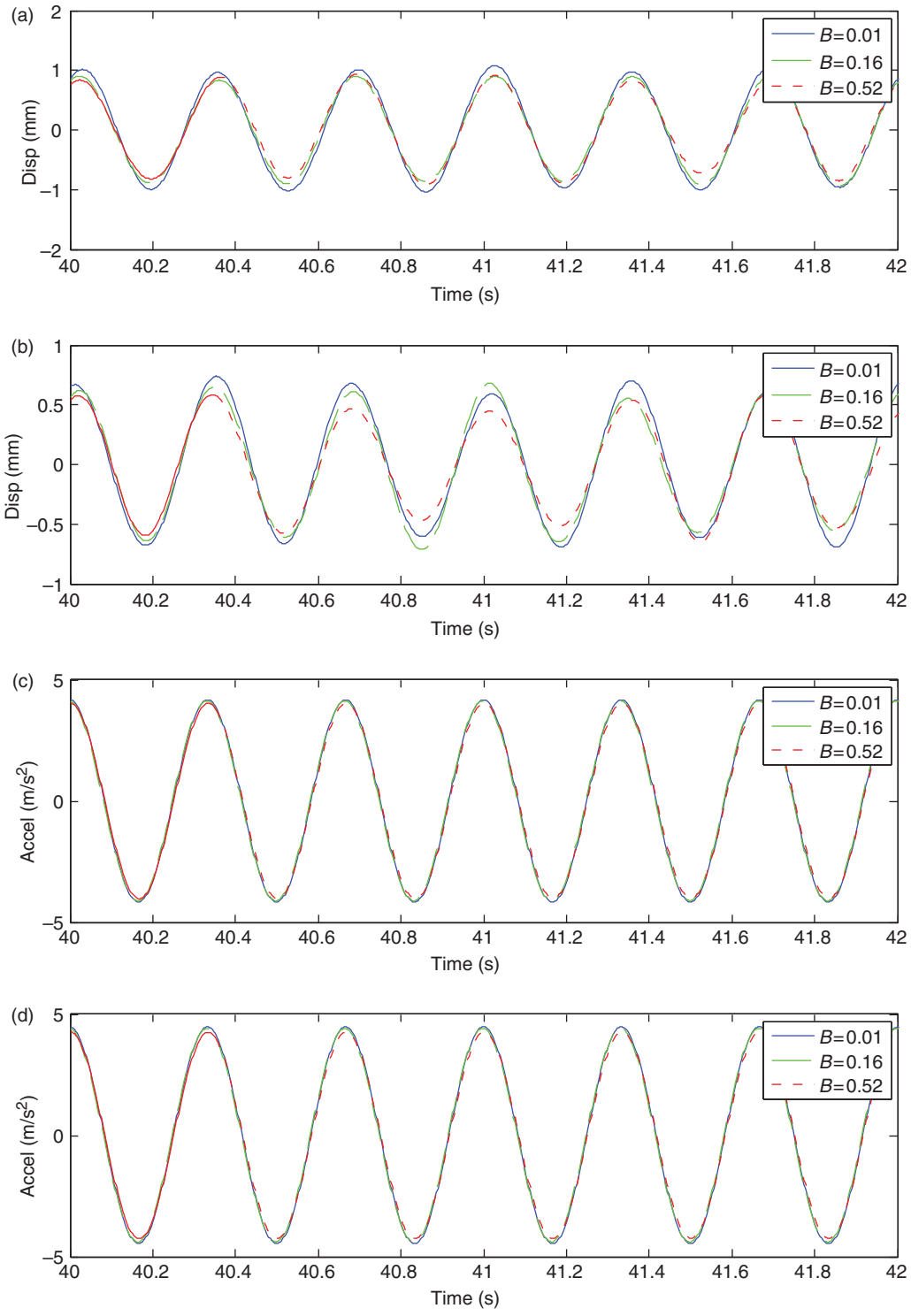

Figure 7. *Structural response in harmonic loading; (a) base drift, (b) structure drift, (c) acceleration at base, and (d) acceleration at top.*

Table 2. Amplitude of structural responses with varying magnetic fields.

	$B = 0.01$ T	$B = 0.16$ T (% reduction)	$B = 0.52$ T (% reduction)
Base drift (mm)	1.05	0.91 (13.33)	0.82 (21.90)
Structure drift (mm)	0.70	0.65 (7.14)	0.58 (17.14)
Accel. at base (m/s^2)	4.17	4.12 (1.20)	4.03 (3.36)
Accel. at top (m/s^2)	4.47	4.41 (1.34)	4.27 (4.47)

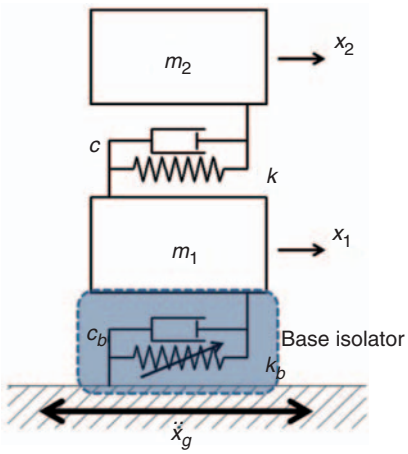

Figure 8. *A 2-DOF building structure model coupled with an MRE base-isolation system.*

Defining the state vectors as $z = \begin{bmatrix} x & \dot{x} \end{bmatrix}^T$ and the output vector to be regulated as $y = \begin{bmatrix} x & \dot{x} & \ddot{x} \end{bmatrix}^T$, the state-space form of the equations of motion can be given by:

$$\dot{z} = Az + Bf + E\ddot{x}_g \tag{6}$$

$$y = C_y z + D_y f + F_y \ddot{x}_g \tag{7}$$

where

$$A = \begin{bmatrix} 0 & I \\ -M^{-1}K & -M^{-1}C \end{bmatrix}, B = \begin{bmatrix} 0 \\ M^{-1}\Lambda \end{bmatrix}, E = \begin{bmatrix} 0 \\ -\Gamma \end{bmatrix}$$

$$C_y = \begin{bmatrix} I & 0 \\ 0 & I \\ -M^{-1}K & -M^{-1}C \end{bmatrix}, D_y = \begin{bmatrix} 0 \\ 0 \\ M^{-1}\Lambda \end{bmatrix} \text{ and}$$

$$F_y = \begin{bmatrix} 0 \\ 0 \\ -\Gamma \end{bmatrix}$$

The state-space equations can be modeled using the MATLB/SIMULINK environment for numerical analysis of the system.

In the numerical simulation, a measured acceleration of shaking table is used as the input excitation to the structure models to simulate the same input loading conditions. To be consistent with the experiment test, the numerical analysis is performed with the three magnetic field cases ($B = 0.01$ T, 0.16 T, and 0.52 T). As shown in Figure 9, the structural responses decrease as the magnetic flux density increases, similar to the experimental results. Table 3 summarizes the amplitude values of the structural responses for the three different test cases.

Comparison between numerical and experimental results

In numerical simulation and experiment test, structural responses have been decreased as magnetic flux density is increased in both cases as shown in Figure 10. It is also observed that the accelerations calculated from numerical simulation match well with those measured from experimental test, whereas the structure drifts calculated from numerical simulation are slightly larger than those measured from experimental test.

Table 4 summarizes the percent difference or the error of the structural responses between the numerical simulation and experiment test results. The numbers are all positive, indicating that the structural responses obtained by the simulations are larger than those of experimental. This may be attributed to the fact that the weight of the structure compresses the MR elastomers in the vertical direction while the materials largely experience shear deformation. The table shows that, by and large, the percent error is small (<10%), except the structure drift responses.

Sesmic performance of the smart base-isolation system

This section presents the seismic performance of the proposed MR elastomer base-isolation system using the numerical model developed in the earlier sections. To regulate the level of stiffness of the MR elastomer element in the system, an adaptive control algorithm needs to be used. In this study, the fuzzy logic-based control is used, because it does not require full-state response information of the entire structure to be implemented, unlike other active control algorithms, such as LQR. Instead, it only needs the displacement and velocity of one of the floors of the structure. Hence, the fuzzy controls might be one of the most viable and practical control algorithms for multiple degree of freedom systems, such as building structures.

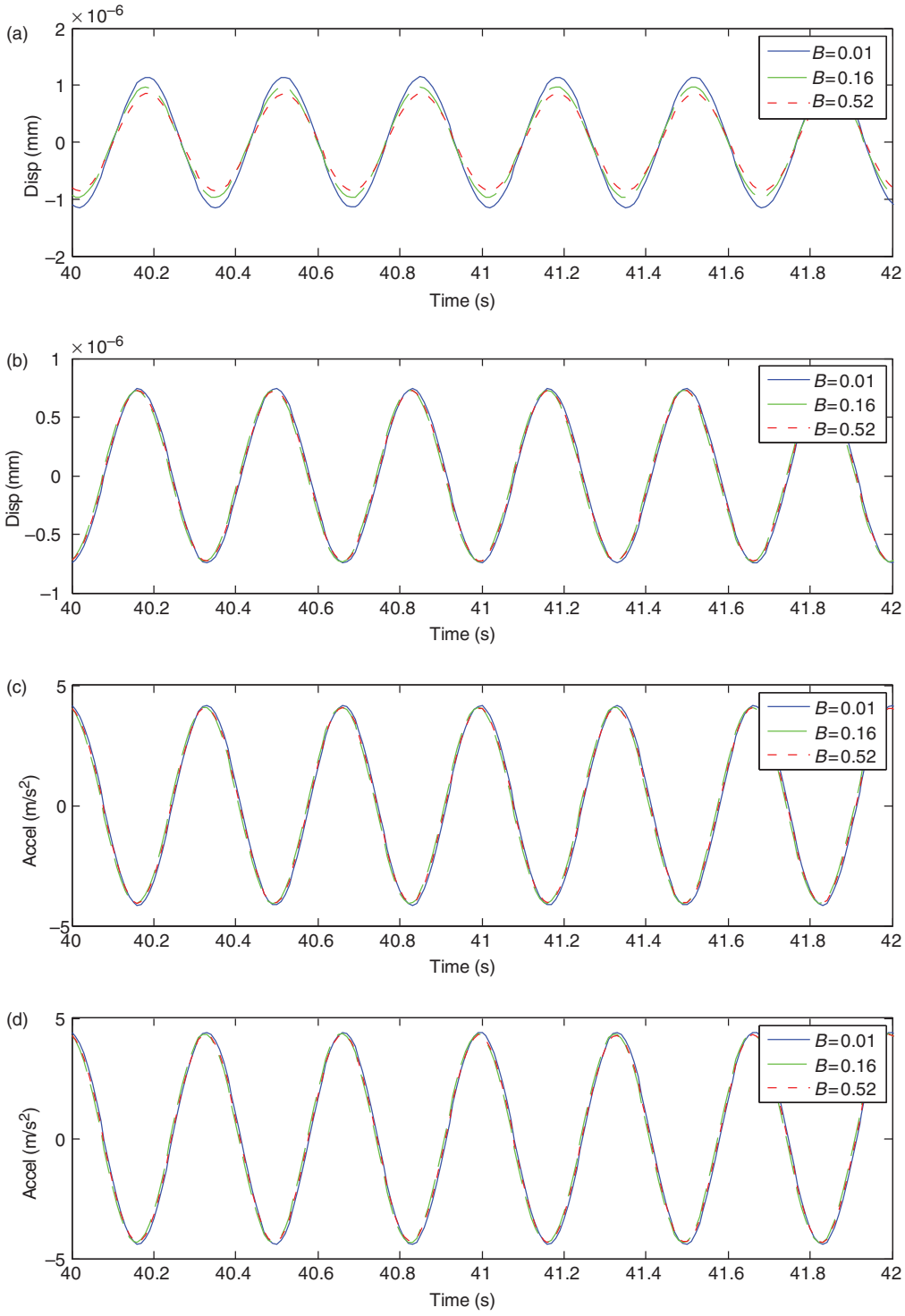

Figure 9. *Structural response in harmonic loading; (a) base drift, (b) structure drift, (c) acceleration at base, and (d) acceleration at top.*

Table 3. Amplitude of structural response.

	***B* = 0.01 T**	***B* = 0.16 T (% reduction)**	***B* = 0.52 T (% reduction)**
Base drift (mm)	1.14	0.96 (15.79)	0.85 (25.44)
Structure drift (mm)	0.74	0.73 (1.35)	0.72 (2.70)
Accel. at base (m/s^2)	4.16	4.08 (1.92)	4.06 (2.4)
Accel. at top (m/s^2)	4.42	4.33 (2.04)	4.31 (2.50)

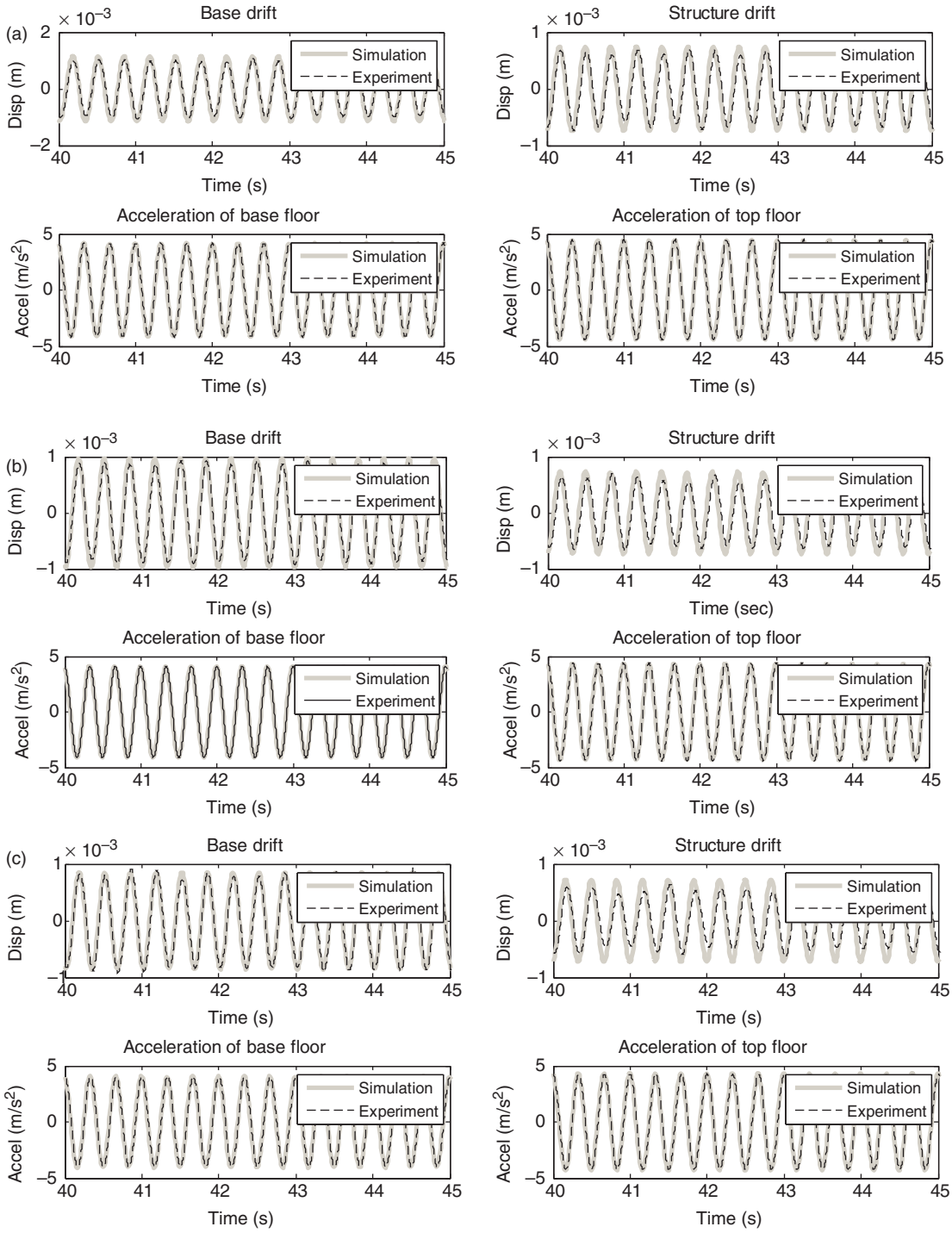

Figure 10. *Comparison between numerical simulation and experiment test; (a) The case of the magnetic flux density of 0.01 T, (b) The case of the magnetic flux density of 0.16 T, (c) The case of the magnetic flux density of 0.52 T.*

Table 4. Error between numerical simulation and experiment test.

	Base drift	Structure drift	Accel. at base	Accel. at top
$B = 0.01$ T (%)	8.57	5.71	0.24	1.12
$B = 0.16$ T (%)	5.21	12.70	0.97	1.81
$B = 0.52$ T (%)	3.66	24.14	0.74	0.94

The fuzzy control algorithm is based on fuzz logic, which is a form of multivalued logic derived from the fuzzy set theory to deal with approximate reasoning. In this study, the relative displacement and velocity of the base of a structure are considered as two input variables for the fuzzy control. Also, the output variable is the magnetic flux density (i.e., B), which will be applied to activate MR elastomers in the isolation system. Gaussian membership functions are used for both input and output variables in the fuzzy control algorithm. Table 5 shows the fuzzy rules. In the table, ''maximum'' means $B = 0.52$ T; on the other hand, ''Zero'' means $B = 0$ T.

To verify the effectiveness of the MR elastomer base-isolation system, a fixed structure (1-DOF model) and a 2-DOF structural model coupled with an equivalent passive base-isolation system are considered. Using an artificial earthquake excitation, which is scaled to the structure, a series of numerical simulations were conducted for the structure model with the fuzzy logic-based control algorithm (Gasparini and Vanmarcke, 1976). Figure 11 shows the artificial earthquake, which is as the input excitation. The structural responses with the control algorithm and without the control (i.e., a conventional or passive-type base isolation system) are compared.

Figure 12 compares the structural responses of the three cases under the earthquake input. It also shows the input magnetic flux density and the control force of the MR elastomer base-isolation system. The peak values of the structural responses are compared in Table 6. In the table, the numbers in the parenthesis show the percent of improvement of the corresponding response with respect to the passive base-isolation case.

Table 5. Fuzzy rules for the smart base-isolation system.

Velocity/Displacement	Negative	Positive
Negative	Maximum	Zero
Positive	Zero	Maximum

Comparing with base isolation, the MR elastomer-based base-isolation shows that maximum value of dynamic responses of a base drift is reduced by 70% and a structure drift is reduced by 40%. As shown in the figure and the table, the both MR elastomer-based control cases show the response reduction as compared with the passive base isolation case, implying the feasibility of the MR elastomers for enhancing the seismic performance of base-isolation systems.

Conclusions

This article investigated the feasibility of the smart base-isolation system based on MR elastomers by numerically evaluating the dynamic performance of the system. In this simulation study, a dynamic model of an MR elastomer base-isolation system, based on the dynamic characteristic test results of MR elastomer samples, was developed, and it was incorporated into a structural model for numerical simulation. For validation purposes, the structural responses of the numerical model were compared with those obtained by the shaking table testing of a shear building model, equivalent to the numerical model, along with MR elastomers. The results indicate that the numerical simulation results are comparable with the experimental results, indicating that the numerical model can adequately represent actual dynamic behaviors of the MR elastomer system. To further investigate the effectiveness of the proposed MR elastomer-based base-isolation system, its dynamic performance (i.e., reducing structural vibrations subject to scaled earthquake excitations) was compared with that of an equivalent fixed structure and a passive base-isolation system. A fuzzy control algorithm was used for changing the stiffness of MR elastomers. The numerical simulation results show that all the responses (base drift, structural acceleration, and interstory drift) of the structure used the smart system based on MR elastomers are smaller than those of the structure used the passive system, indicating that the MR elastomer-

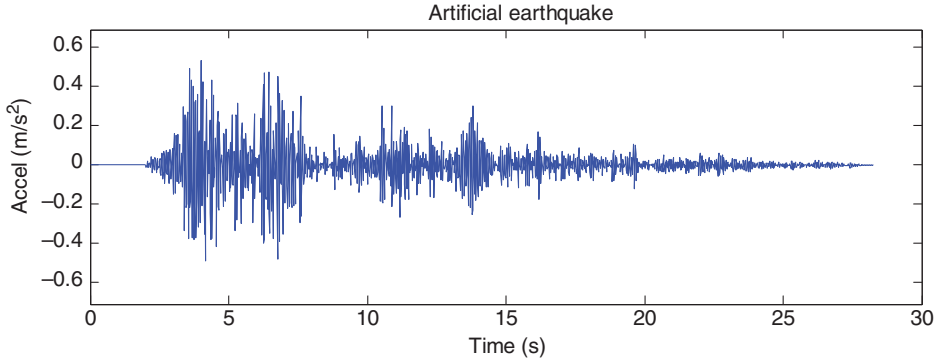

Figure 11. *Input excitation (artificial earthquake).*

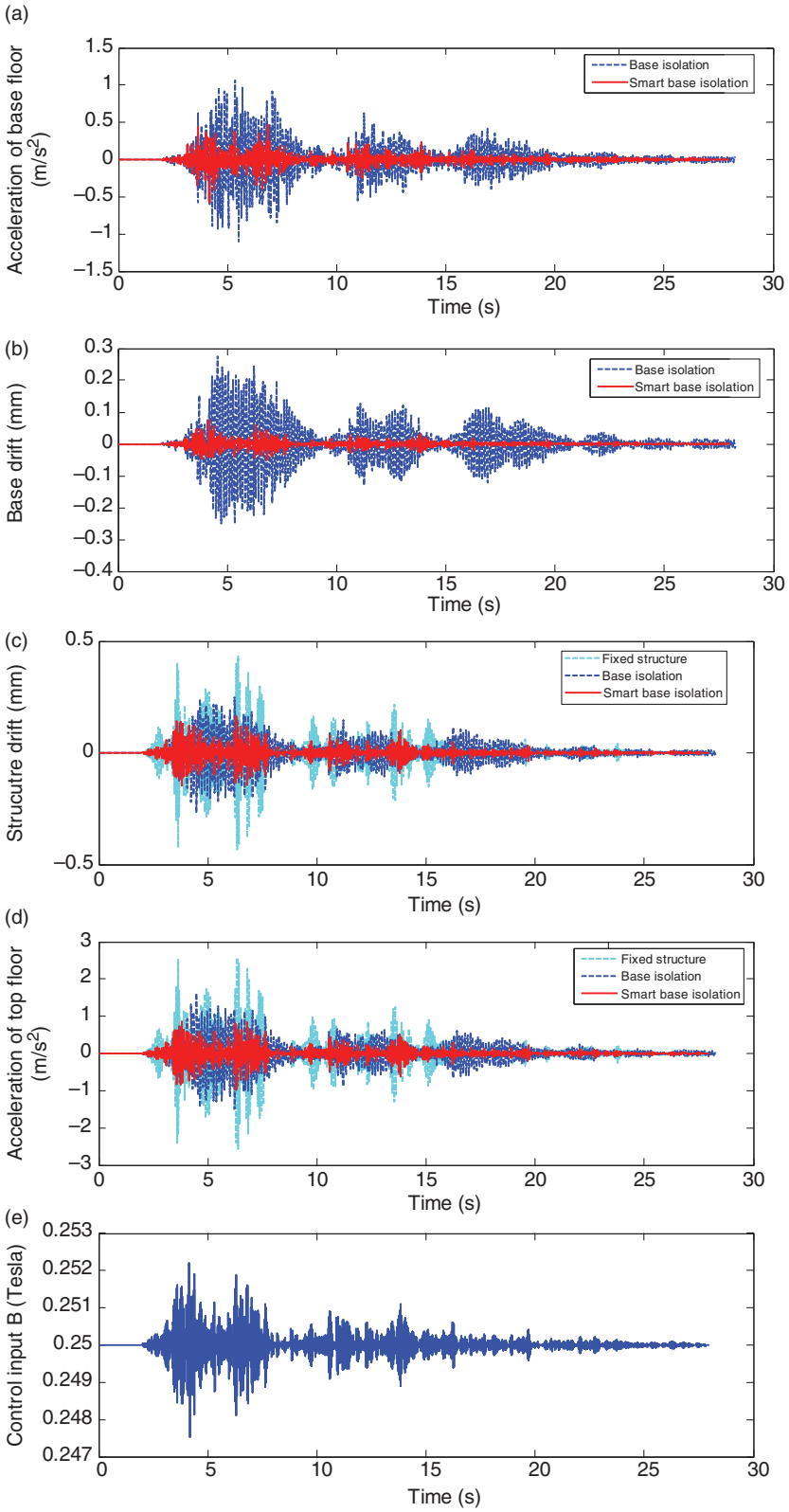

Figure 12. *Structural responses of 2-DOF structure for earthquake case: (a) base drift (mm), (b) structure drift (mm), (c) structure acceleration of base floor (m/sec^2), (d) structure acceleration of top floor (m/sec^2), (e) MR elastomer input magnetic flux density (T), and (f) control force (N).*

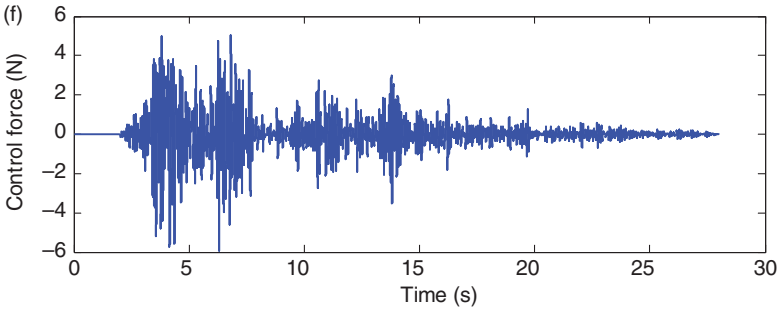

Figure 12. *Continued.*

Table 6. Maximum structural responses in the earthquake case.

	Fixed structure	Base isolation	Smart base isolation (% improvement)
Base drift (mm)	–	0.27	0.08 (70.37)
Structure drift (mm)	0.43	0.27	0.16 (40.74)
Acceleration at base (m/sec^2)	–	1.11	0.57 (48.65)
Acceleration at top (m/sec^2)	2.57	1.61	0.98 (39.13)

based system outperformed its passive counterpart. Therefore, it is feasible that the smart base-isolation system using MR elastomers could be used as an alternative base isolator for improving the seismic protection of base isolated structures. However, more extensive researches should be performed, numerically as well as experimentally, before applying MR elastomers in large engineering structures, such as high-rise buildings and long-span bridges. As a future study, additional experimental tests will be conducted using a larger scale MR elastomer base-isolation systems and/or a multiple degree of freedom structure. Moreover, new control algorithms suitable for the MR elastomer systems will be investigated.

Acknowledgement

This work was partly supported by the Nuclear Research & Development of the Korea Institute of Energy Technology Evaluation and Planning (KETEP) grant funded by the Ministry of Knowledge Economy, Republic of Korea (No. 2010T100101085) and the IT R&D program of MKE/IITA [2008-F-044-01, Development of new IT convergence technology for smart building to improve the environment of electromagnetic waves, sound and building]. Their financial supports are gratefully acknowledged.

References

Deng, H.X. and Gong, X.L. 2007. "Adaptive tuned vibration absorber based on magnetorheological elastomer," *J Intell Mater Syst Struct*, 18:1205–1210.

Faycal, I., Victor, M. and Jose, R. 2007. "Dynamic properties of the hysteretic Bouc-Wen model," *Syst Control Lett*, 56:197–205.

Gasparini, D. and Vanmarcke, E.H. 1976. "*A Program for Artificial Motion Generation*," *Department of Civil Engineering*. Cambridge, MA: Massachusetts Institute of Technology.

Mendoza, M.J. and Auvinet, G. 1988. "The Mexico earthquake of september 19, 1985-behavior of building foundations in Mexico city," *Earthquake Spectra*, 4:835–853.

Mohammed, I., Faycal, I. and Jose, R. 2009. "The hysteresis Bouc-Wen model, a survey," *Arch Comput Methods Eng*, 16:161–188.

Jung, H.J., Lee, S.J., Jang, D.D., Kim, I.H., Koo, J.H. and Khan, F. 2009. "Dynamic characterization of magneto-rheological elastomers in shear mode," *IEEE Trans Magn*, 40:3930–3933.

Koo JH, Sung, SH, Lee, HJ and Jung, HJ 2008. Seismic protection of structures using smart base isolation systems based on MR elastomers. In: *Proceedings of the 4th International Conference on Advances in Structural Engineering and Mechanics (ASEM08)*, Jeju, Korea.

Opie, S. and Yim, W. 2009. "Design and control of a real-time variable stiffness vibration isolator," In: *Proceedings of 2009 IEEE/ASME International Conference on Advanced Intelligent Mechatronics*, Singapore.

Ramallo, J.C., Johnson, E.A. and Spencer Jr, B.F. 2002. "Smart' base isolation systems," *J Eng Mech, ASCE*, 128:1088–1099.

Spencer Jr, B.F. and Nagarajaiah, S. 2003. "State of the art structural control," *J Struct Eng, ASCE*, 129:845–856.

Wang, Y.L., Hu, Y., Gong, X.L., Jiang, W.Q., Zhang, P.Q. and Ghen, Z. 2006. "Preparation and properties of magnetorheological elastomers based on silicon rubber/polystyrene blend matrix," *J Appl Polym Sci*, 103:3143–3140.

Yoshioka, H., Ramallo, J.C. and Spencer Jr, B.F. 2002. "Smart' base isolation strategies employing magnetorheological damper," *J Struct Eng ASCE*, 128:540–551.